

MOL 46664

1

Anti-inflammatory, antiproliferative, and cytoprotective activity of NO chimera nitrates of use in cancer chemoprevention

Ghenet K. Hagos, Samer O. Abdul-Hay, Johann Sohn, Praneeth D. Edirisinghe, R. Esala P. Chandrasena, Zhiqiang Wang, Qian Li, Gregory R.J. Thatcher

Department of Medicinal Chemistry & Pharmacognosy,
College of Pharmacy,
University of Illinois at Chicago,
Chicago,
IL 60612

Running Title: In vitro activity of nitrates of use in chemoprevention

Text pages: 35

Tables: 0

Figures: 10

References: 50

Abstract: 219 words

Introduction: 500 words (excluding citations)

Discussion: 1500 words (excluding citations)

Abbreviations: ARE, antioxidant responsive element; BF, 4'-bromoflavone; CD, concentration required to double the specific activity of NQO1; CI, chemopreventive index = IC_{50}/CD ; DCM, dichloromethane; NO-NSAID, NO donating NSAID; NSAID non-steroidal anti-inflammatory drug; NQO1, NAD(P)H-dependent quinone oxidoreductase; ASA, aspirin; CRC, colorectal cancer; ACF, aberrant crypt foci; AOM, azoxymethane; LPS, lipopolysaccharide; TNF- α , tumor necrosis factor- α ; IL, interleukin; COX, cyclooxygenase; iNOS, inducible isoform of nitric-oxide synthase; PGs, prostaglandins; MAPK, mitogen-activated protein kinase; ERK, extracellular signal-regulated kinase

ABSTRACT

Non-steroidal anti-inflammatory drugs (NSAIDs) have shown promise in colorectal cancer (CRC), but are compromised by gastrotoxicity. NO-NSAIDs are hybrid nitrates conjugated to an NSAID designed to exploit the gastroprotective properties of NO bioactivity. The NO chimera, GT-094, a novel nitrate containing an NSAID and disulfide pharmacophores, is effective in vivo in rat models of CRC and is a lead compound for design of agents of use in CRC. Preferred chemopreventive agents possess: (1) antiproliferative and (2) anti-inflammatory actions; and (3), the ability to induce cytoprotective phase 2 enzymes. To determine the contribution of each pharmacophore to the biological activity of GT-094, these 3 biological activities were studied in vitro in compounds that deconstructed the structural elements of the lead, GT-094. The anti-inflammatory and antiproliferative actions of GT-094 in vivo were recapitulated in vitro; and, GT-094 was seen to induce phase 2 enzymes via the antioxidant response element (ARE). In the variety of colon, macrophage-like, and liver cell lines studied, the evidence from structure-activity relationships was that the disulfide structural element of GT-094 is the dominant contributor in vitro to the anti-inflammatory activity, antiproliferation, and enzyme induction. The results provide a direction for lead compound refinement. The evidence for a contribution from the NO mimetic activity of nitrates in vitro was equivocal and combinations of nitrates with ASA were inactive.

INTRODUCTION

Colorectal cancer (CRC) is a leading cause of death, providing impetus for discovery of new chemopreventive agents. Chemoprevention strategies for CRC have targeted antiproliferative and anti-inflammatory actions on colonocytes containing populations subject to carcinogen induced DNA damage. Although, the exact mechanisms of colon carcinogenesis remain to be revealed, there are clear biomarkers that correlate with drug intervention and tumorigenesis, in particular biomarkers of inflammation and of proliferation.

Aberrant crypt foci (ACF) are seen as an early precursor stage to adenomas and cancer, which facilitate early diagnosis. The ACF is a monoclonal structure that arises from mutations within a single crypt stem cell, thought to result from a single mutational event within an isolated colon crypt. ACF are strongly linked to colon cancer risk, and in animal models, such as the murine azoxymethane (AOM) carcinogen model, a good correlation between ACF number and tumorigenesis has been reported for a variety of chemopreventive agents (Corpet and Tache, 2002). ACF are a reliable biomarker for colon cancer in preclinical models and are of use in drug discovery. Furthermore, in humans, ACF demonstrate increased expression of markers of proliferation, and inflammation (e.g. inducible NO synthase; iNOS) (Hao et al., 2001).

Non-steroidal anti-inflammatory drugs (NSAIDs), such as acetylsalicylic acid (ASA, aspirin), have shown promise in CRC clinical trials (Rosenberg et al., 1998). However, chronic NSAID use has fatal side effects from severe gastrointestinal (GI) damage, and their efficacy at low doses in CRC is problematic. Exploration of the use of NO-NSAIDs (nitric oxide donor NSAIDs) in CRC represented a logical progression, because NO-NSAIDs were originally designed to deliver the biological activity of NO to mollify the GI damage caused by NSAIDs. The most widely studied NO-NSAID, NCX 4016, is an NO-ASA that entered NCI-sponsored

clinical trials for CRC prevention having shown promise in preclinical studies (Bak et al., 1998; Rao et al., 2006).

NO-NSAIDs are hybrid nitrate drugs; aliphatic nitrates conjugated via a labile ester linkage to an NSAID (Bolla et al., 2005). Nitrates, themselves, have been in clinical use for over 130 years in cardiovascular therapy (Thatcher, 2007; Thatcher et al., 2004). There is a substantial body of work on NO-ASA related to CRC, however, key gaps in our knowledge have been highlighted by Rigas and co-workers (Kaza et al., 2002), and importantly, structural optimization of NO-NSAIDs specifically for CRC chemoprevention has not been explored. The NCX 4016 Phase 2 CRC chemoprevention clinical trial was recently halted because of potential drug toxicity amplifying the need for a deeper understanding of structure activity relationships. It is possible that drug optimization of a nitrate-NSAID hybrid for CRC would circumvent the toxicity reported for NCX 4016.

The novel nitrate, GT-094, in simile with NO-NSAIDs, contains an NSAID and a nitrate, but also a disulfide pharmacophore, known to be effective in chemoprevention. GT-094 was validated as a lead compound for chemoprevention by studies in the rat/AOM model of human CRC, which demonstrated significant reductions in ACF number and several biomarkers linked to CRC (Hagos et al., 2007). In this paper, GT-094 is studied *in vitro* and the pharmacophore elements are structurally deconstructed to gain insight into the relationship of structure to anti-inflammatory, antiproliferative, and cytoprotective activity. The results impact future development strategies for optimization of nitrate-NSAID hybrid drugs for CRC.

MATERIALS & METHODS

Materials: Full synthesis and characterization data for novel compounds is presented in Supplemental Information. BECS (1,2-bis-(2-ethoxycarbonylphenyl)sulfane), NCX 4016, GT-015 and GT-094, all previously described, were synthesized by minor modification of literature procedures, purified, and fully characterized (Hagos et al., 2007; Nicolescu et al., 2002). Buffered formalin, xylene, and alcohols (histology grade) were from Fisher Scientific (Pittsburgh PA). All other biochemical reagents were from Sigma (St. Louis, MO).

Biology: Caco-2 human colonic adenocarcinoma cells obtained from ATCC were grown in Dulbecco's Modified Eagle Medium (DMEM)/F-12 supplemented with 1% penicillin-streptomycin, 20% fetal bovine serum, nonessential amino acids, sodium pyruvate, 1.5g/L sodium bicarbonate and incubated in 5% CO₂ at 37 °C. HT-29 human adenocarcinoma cells were supplied by Dr. Genoveva Murillo (IIT Research Institute, Chicago, IL). Cells were maintained in RPMI 1640 medium, supplemented with 1% antibiotic-antimycotic, 1% L-glutamine (200mM), 10% fetal bovine serum (Atlanta Biologicals, Atlanta, GA), and incubated in 5% CO₂ at 37 °C. RAW 264.7 mouse macrophage-like cells, provided by Dr. J. Cook (UIC, Chicago, IL), were maintained in Dulbecco's Modified Eagle Medium (DMEM) supplemented with 1% penicillin-streptomycin, 10% fetal bovine serum and incubated in 5% CO₂ at 37 °C. The mouse alveolar macrophage MH-S cell line was a generous gift from Dr J. Cook (UIC, Chicago). MH-S cells were maintained in RPMI 1640 medium containing 10% fetal bovine serum and 1% penicillin/streptomycin/amphotericin. Hepa 1c1c7 murine hepatoma cells were supplied by Dr. J.P. Whitlock, Jr. (Stanford University, Stanford, CA) and were cultured in α -MEM with 1% penicillin-streptomycin and 10% fetal bovine serum (Atlanta Biologicals, Atlanta, GA). HepG2 cells stably transfected with ARE-luciferase reporter gene were kindly provided by Dr. A.N. Kong (Rutgers University, Piscataway, NJ) and cultured in F-12 medium with 10% fetal bovine

serum, 1% penicillin-streptomycin, 1% non-essential amino acids and 0.2 mg/mL insulin (Chen et al., 2000). MCF-7 WS8 human breast cancer cells (a kind gift from Dr. V. C. Jordan, Fox Chase Cancer Center, Philadelphia, PA) were maintained in RPMI 1640 containing 10% fetal bovine serum (FBS; Atlanta Laboratory, Atlanta, GA), 2 mM L-glutamine, 0.1 mM nonessential amino acids, and 6 µg/mL bovine insulin (Sigma). Estrogen-free media were prepared by supplementing 3x dextran-coated charcoal-treated FBS to phenol-red free RPMI 1640 media while other components remained the same. Assays were performed in at least two separate cell passages.

Proliferation assay: Cells were seeded in 96-well plates at a density of 2×10^4 cells/mL in 190 µL media. After 24 h incubation, test samples were added to each well and the cells incubated for an additional 24, 48, or 96h. The cells were fixed by adding ice cold 20% trichloroacetic acid and incubated for 30 min at 4°C. The plates were then washed with water and air-dried. The trichloroacetic acid fixed cells were stained with 100 µL of 0.4% sulforhodamine B (SRB) and incubated for 30 min at room temperature. The free dye was washed with 1% aqueous acetic acid and the plates were air dried. The bound dye was solubilized by adding Tris base (10 mM, 200µL). The plates were placed on an orbital shaker (100 rpm) for 10 min at room temperature. The absorption was measured at 515 nm, using a plate reader and normalized to control cells.

Griess assay: Macrophage cells were plated at a concentration of 12×10^4 cell/mL (or as otherwise stated in text and figure captions) in a 96 well plate. Cells were plated in DMEM and incubated at 37°C for 24 h. The medium was changed, allowing cell induction by addition of LPS (lipopolysaccharide from E. coli 055:B5; Sigma, St Louis, MO) in the medium. Test compounds were added, and at the indicated time points, 100µL of the supernatant was removed and incubated with the Griess reagent (100µL; 0.5% sulfanilamide, 0.05% (N-1-

naphthyl)ethylenediamine dihydrochloride, 2.5% H₃PO₄ and 97% H₂O by weight) for 30 min at room temperature in the dark. The absorbance was measured at 530 nm on a Dynex MRX II microplate spectrophotometer and calibrated using a standard curve constructed with sodium nitrite to yield NO₂⁻ concentration. Where indicated in the text, subtraction of NO₂⁻ formed in cell incubations of nitrates in the absence of LPS, was used to determine NO₂⁻ production from endogenous NOS mediated production of NO.

In preliminary experiments with the NOS inhibitor in RAW 264.7 cells: cells were plated at a concentration 25 x 10⁴ cell/well in a 24 well plate for 24 h; L-NAME (10μM) was added; after a further 40 min, cells were induced with LPS (1 μg/ml); after 24 h, 50 μL of the supernatant was withdrawn and analyzed in the Griess assay using calibration curves obtained under identical conditions. For assay using conditioned media (CM) from non-induced and LPS-induced RAW 264.7 cell cultures, cells were cultured as above and incubated for 12 h in the absence and presence of LPS and L-NAME. Aliquots of supernatant were removed to a 96 well plate and further incubated for 12 h with or without GT-094 (100 μM) before Griess assay.

In experiments to study the effect of cell density and of arginine depletion, RAW 264.7 cells were plated at either 5x10⁴, 10x10⁴, or 20x10⁴ cells/well for 24 h; media was replaced with FBS free media containing GT-094 (100 μM); after a further 30 min LPS (1ug/ml) was added and cells incubated for 20 h before collection of supernatant aliquots for Griess assay. For study of arginine depletion, cells were plated at 20x10⁴ cells/well and after 24 h the media was replaced with FBS free media (obtained from AthenaES, Baltimore MD) containing or absent L-arginine. GT-094 (100 μM) was immediately added, followed after 30 min by LPS. The Griess assay was performed after 20 h incubation.

Immunoblot analysis: Cells were plated 400-500x10⁴ cells/dish in 100mm dishes. After 24h cells were treated with the test compounds at the desired concentrations. After the desired

time period, cells were lysed as follows: media was removed and cells were washed twice with ice cold PBS followed by addition 250 μ L of ice cold 1x lysis buffer (Cell Signaling Technology, #9803, Danvers, MD). Cells were scraped with the lysis buffer and transferred into an eppendorf tube and left on ice for 30 min while vortexing occasionally. The tubes were centrifuged at 12000 g for 15 min and the supernatant transferred into a fresh tube and stored at -80°C. Protein concentrations were determined using a standard protein assay kit (Bio-Rad, Hercules, CA). Proteins were separated by 8% SDS gel, and then transferred to polyvinylidene difluoride (PVDF) membrane. The membrane was incubated with the desired primary antibody (p53, phospho-p53, pERK, ERK from Cell Signaling Technology; iNOS from Santa Cruz Biotechnology, Santa Cruz, CA; actin from Sigma) in 3% w/v nonfat dry milk in buffer, and incubated with the secondary antibody (anti-rabbit IgG or anti-mouse IgG) conjugated with horseradish peroxidase (Cell Signaling Technology) in 3% w/v nonfat dry milk in buffer. Immunoreactive proteins were detected by chemiluminescence (Santa Cruz Biotechnology reagents) and visualized after exposure to a Kodak Biomax film.

NQO1 activity assay: Induction of NQO1 activity was assessed in Hepa 1c1c7 murine hepatoma cells as described previously with minor modifications (Prochaska and Santamaria, 1988). Briefly, Hepa 1c1c7 cells were seeded in 96-well plates at a density of 1.25×10^4 cells/mL in 190 μ L media. After 24 h incubation, test samples were added to each well and the cells incubated for a further period of time (0-24 h). The medium was decanted and the cells incubated at 37 °C for 10 min with 50 μ L of 0.8% digitonin and 2 mM EDTA solution (pH 7.8). The plates were then agitated on an orbital shaker (100 rpm) for 10 min at room temperature, and 200 μ L of reaction mixture (0.7 mg/mL bovine serum albumin (BSA), 0.3mg/mL (3-(4,5-dimethylthiazo-2-yl)-2,5-diphenyltetrazolium bromide) (MTT), 25 mM Tris-HCl, 0.01% Tween 20, 5 μ M FAD, 1 mM glucose-6-phosphate, 30 μ M NADP, 2 U/mL glucose-6-phosphate

dehydrogenase, and 50 μ M menadione) was added to each well. After agitation on a shaker for 5 min, the plates were scanned at 595 nm. The specific activity of NQO1 was determined by measuring NADPH-dependent menadiol-mediated reduction of MTT to blue formazan. Induction of NQO1 activity was calculated by comparing the NQO1 specific activity of sample-treated cells with that of solvent-treated cells. CD values represent the concentration required to double NQO1 induction. The Chemopreventive Index (CI= IC_{50}/CD) is calculated from IC_{50} for inhibition of cell growth (Song et al., 1999), which was measured for Hepa 1c1c7 cells by decanting medium from 96 well plates, followed by addition of 200 μ L of 0.2% crystal violet (CV) solution in 2% ethanol. After 10 min the plates were rinsed for 2 min with water and dried. The bound dye was solubilized by incubation at 37°C for 1 h with 200 μ L of 0.5% SDS in 50% ethanol. The absorption of CV was measured at 595 nm.

RT-PCR analysis: RAW 264.7 cells were plated at a concentration of 400×10^4 cells/mL in a 100 mm dish. After 24 h cells were treated with GT094 and 1 μ g/mL LPS. After 4 h, media was removed and cells were washed with PBS and lysed by adding Trizol (Invitrogen, Carlsbad, CA). Cells were scraped and transferred into eppendorf tubes; chloroform (200 μ L) was added and vortexed at room temp. The tubes were centrifuged at 12000rpm for 10 min at room temperature and the supernatant (~600 μ L) was transferred to a new tube, and 1x volume (~600 μ L) of isopropanol was added. The tubes were left at -20°C for 30 min and centrifuged at 14000rpm at 4°C for 15 min. The supernatant was discarded and the pellets were washed with 70% ethanol (1mL), centrifuged at 14000 rpm for 10 min and ethanol was removed and the pellets left for 1-2 min to dry. The pellets were dissolved in DEPC treated water (Ambion, Austin, TX). OD was measured at 260/280 nm to determine the concentration of RNA. Total RNA (5 μ g) was reverse transcribed by using SuperScript II RT, dNTP and oligo(dT)₁₂₋₁₈ as described in the manufacturers protocol (Invitrogen, Carlsbad, CA). cDNA (2 μ L) was amplified

by PCR. PCR reactions were carried out in a volume of 50 μ L containing Taq DNA polymerase (5U/mL), 0.2mM dNTP, 1x reaction buffer, and 200 pmol of 5' and 3' primers (Operon Biotechnologies, Huntsville, AL; see Supplemental Information for details). After one cycle of denaturation, amplification cycles were performed for TNF α , IL-1 β , IL-6, iNOS, and COX-2: 1 min of 94 $^{\circ}$ C denaturation; 1 min of 60 $^{\circ}$ C annealing; and 1 min 72 $^{\circ}$ C extension. After amplification, electrophoresis was performed on 1% agarose gel and visualized by ethidium bromide staining and UV light.

Prostaglandin analysis. After plating for 24 h, RAW 264.7 cells were treated with GT094 at different concentration and 1 μ g/mL LPS was added after 30 min. After a further 24 hr, media was collected and analyzed for prostaglandins. 1N citric acid (40 μ L) and 10% BHT (5 μ L) were added immediately to inhibit oxidation. Prior to extraction 20 μ l of PGE₂-d₄ (100 ng/ml) was added to each sample as an internal standard. Prostaglandins were extracted from cell suspensions by adding 2 ml of hexane:ethyl acetate (1:1, v/v) and vortex mixing for 2 min. Samples were centrifuged (1800g for 10 min at 4 $^{\circ}$ C) and the upper organic layer was then transferred to a glass test tube on ice. The extraction step was repeated twice and the organic phases evaporated to dryness under a stream of nitrogen at room temperature. All extraction procedures were performed under low light and low temperature conditions to minimize potential photooxidation or thermal degradation of eicosanoid metabolites. Samples were reconstituted in 200 μ l methanol prior to LC/MS/MS analysis (Yang et al., 2002). LC/MS/MS was performed using an API 3000 mass spectrometer (Applied Biosystem, Foster City, CA, USA) equipped with an Shimadzu HPLC (Kyoto, Japan). Prostaglandins were chromatographically resolved using a Luna 3- μ m, phenylhexyl, 2 x 150-mm analytical column (Phenomenex, Torrance, CA) using a methanol/ammonium acetate (10 mM, pH 8.5) gradient at

a flow rate of 400 $\mu\text{L}/\text{min}$. Individual analytes were detected and quantified according to the literature (Yang et al., 2002).

RESULTS

Chemistry. 7 synthetic compounds were selected, containing various structural elements, for comparison with the parent, GT-094, and both ASA, and the classical nitrate, ISDN (Fig. 1). Efficient synthesis of dinitrates requires oxidative nitration procedures which inherently are not compatible with oxidizable functional groups such as sulfides, therefore a new synthesis was developed to allow access to dinitrates GT-794 and GT-974.

Antiproliferative activity. The in vivo antiproliferative activity of GT-094 in the colon in the rat/AOM model of CRC was reported previously (Hagos et al., 2007). In two human colon cancer cell lines studied herein, Caco-2 and HT-29, GT-094 was not cytotoxic at the concentrations studied ($\leq 100 \mu\text{M}$), but was antiproliferative with measured IC_{50} of $41 \mu\text{M}$ (Fig. 2A) and $59 \mu\text{M}$, respectively. Similarly, the disulfanyl tetranitrate, GT-015, and the disulfanyl bis-thiosalicylate, BECS, significantly inhibited growth of Caco-2 and HT-29 cells (Figs 2B, C). GT-094 showed similar antiproliferative potency in RAW 264.7 cell culture in the absence of added LPS ($\text{IC}_{50} = 51 \mu\text{M}$; Fig. 2C). BECS inhibited cell growth more potently than GT-094, and both GT-749 and GT-947, analogs of GT-094 missing only the disulfide pharmacophore, decreased cell growth by 50% at $100 \mu\text{M}$ (Fig. 2D), suggesting that the sulfanyl nitrate element possesses antiproliferative properties, but weaker than those of the disulfide element.

Anti-inflammatory activity: iNOS induction and NO release. The murine macrophage-like RAW 264.7 cell line is routinely used to examine the ability of agents to block cellular inflammatory response, and represents a model for anti-inflammatory action towards activated macrophages. Treatment with the bacterial endotoxin LPS reliably induces various cytokines and also triggers expression of iNOS, the activity of which is readily assessed by measurement of inorganic nitrite (NO_2^-). Although not a direct measure of NO production, NO_2^- is a major product of NO oxidative metabolism which can readily be quantified using the Griess

assay. However, the majority of nitrates undergo denitration to NO_2^- as the major product (Thatcher et al., 2004). Therefore to quantify endogenous NO_2^- production due to iNOS activity, NO_2^- production from nitrate test compounds must be accounted for.

In non-induced, untreated cells, no significant basal NO_2^- was detected, whereas ISDN (100 μM) treated cells accumulated $2.7 \pm 0.5 \mu\text{M NO}_2^-$, and cells treated with GT-094 (10, 50, 100 μM) generated 3.4 ± 0.2 , 16.2 ± 0.3 , and $38.7 \pm 0.7 \mu\text{M NO}_2^-$, respectively (Fig. 3B). ASA had no influence on NO_2^- release from ISDN, and no increase in NO_2^- production from ISDN or GT-094 was seen from 12 h to 24 h. A more complete time course of NO_2^- release was measured for GT-015 compared to the true NO donor, SPE/NO (Fig. 3 A). In non-induced cells, SPE/NO (100 μM) gave NO_2^- (97 μM) within 5 h. This represents 50% of the maximum theoretical yield of NO_2^- from SPE/NO (Maragos et al., 1991), given the theoretical 1:1 conversion of NO to NO_2^- from autoxidation (Ford et al., 1993). This yield of NO_2^- compares with 30-40% of the maximum theoretical yield of NO_2^- produced from denitration of GT-094 in incubations with non-induced cells (Fig. 3B). Since these are not sealed systems, loss of NO by effusion is expected. Interestingly, it was further observed that denitration of GT-094 occurred to a substantial extent in cell culture supernatant drawn from both induced and non-induced RAW 264.7 cells (Fig. 4).

The proposed methodology to quantify endogenous NO_2^- production by iNOS, measures NO_2^- release in induced cells and subtracts the NO_2^- levels observed in non-induced cells. If hypothetically, denitration of GT-094 was modified in LPS induced cells, this methodology would be problematic. Therefore, the denitration of GT-094 was further studied in RAW 264.7 cells, in which endogenous NO_2^- production was attenuated, using the NOS inhibitor, L-NAME, or media absent the NOS substrate, L-arginine. The NOS inhibitor, L-NAME (10 μM) inhibited NO_2^- production by $46.1 \pm 3.5\%$ at 24 h in LPS induced RAW 264.7 cells. The denitration of

GT-094 was measured in supernatants from RAW 264.7 cells incubated with or without LPS and L-NAME (Fig. 4). The results demonstrated that LPS induction did not have a significant effect upon the amount of NO_2^- produced by GT-094; that GT-094 was stable to denitration in culture media, and that denitration was efficient in the presence of factors expressed by both induced and non-induced cells. These observations suggested that the reactivity of GT-094 would be dependent upon cell density. This was confirmed by measurement of NO_2^- production from GT-094 (100 μM) as a function of cell density (Fig. 5A). In media depleted of L-arginine, LPS induction of iNOS does not result in NO or NO_2^- production (Fig. 5B). Categorically, this experiment shows that factors induced by LPS in RAW 264.7 cells do not influence GT-094 denitration. The methodology proposed is therefore sound, with the caveat that both GT-094 reactivity and iNOS induction are dependent on cell density.

The time course for generation of NO_2^- from induced RAW 264.7 cells (Fig 6A) was thus corrected using our methodology to yield endogenous NO_2^- produced by iNOS (Fig. 6B). The observed time course for endogenous production of NO_2^- from RAW 264.7 cells in response to LPS stimulation is entirely compatible with literature reports describing the time course of iNOS induction (Connelly et al., 2001). By measuring NO_2^- at 24 h in cell culture with and without LPS, and correcting for background release, the anti-inflammatory activity towards iNOS induction was compared for the variety of compounds selected to provide structural elements of GT-094 (Fig. 6C; and see Fig. 1). The classical nitrates, ISDN and GTN, had negligible effects on LPS-induced elevation of NO_2^- . The disulfides BECS, GT-015 and GT-094 in a concentration dependent manner, substantially inhibited NO_2^- production. However, the sulfanyl nitrate, GT-794 was without effect; GT-794 differs from GT-094 in only one S atom; it is identical in every structural element, except for the disulfide. ASA had no effect on NO_2^- production; and NO_2^- itself, which is clearly a major breakdown product of GT-015 and GT-094,

did not inhibit endogenous NO_2^- production. The ISDN drug combinations (at the same concentrations delivered singly) had little additive activity of note on NO_2^- production.

The observations in RAW 264.7 cells with the true NO donor, SPE/NO demonstrated that NO at low concentrations stimulated iNOS expression and NO_2^- production, but at high concentrations modestly inhibited NO_2^- formation. The first observation is compatible with a proposed role for NO from eNOS early in macrophage activation (Connelly et al., 2003), the second with proposed negative feedback, or autoinhibition of iNOS induction by higher levels of iNOS-derived NO (Hinz et al., 2000). To confirm the generality of the observations on RAW 264.7 cells, the alternative MH-S macrophage cell line was studied with GT-015 and SPE/NO, measuring NO_2^- production; confirming the observations on RAW 264.7 cells (Fig. 6C).

To further explore the GT-094 reactivity, the capacity of denitration to yield NO was studied using protein phosphorylation in MCF-7 cells as a sensitive cellular NO sensor. Thomas et al. exhaustively explored this cell model system using NONOates to generate various fluxes of NO: phosphorylation of p53 and of ERK was shown to be a sensor for intracellular NO, responding to true NO donors in a time and concentration dependent manner: p53 phosphorylation required higher concentrations of NO, whereas ERK was phosphorylated at lower concentrations (Thomas et al., 2004). Incubation of cells with GT-094 (100 μM) did not increase levels of phospho-p53 with time, in contrast to the true NO donor, SPE/NO (100 μM); whereas, both GT-094 (100 μM) and SPE/NO (10 μM) gave ERK phosphorylation (Fig. 7). The interpretation of these data is that GT-094 may function as a cellular NO donor, but the fluxes of NO produced are not high.

Anti-inflammatory activity and PG release. Western blots of lysates from RAW 264.7 cells confirmed that GT-094 blocked iNOS protein expression rather than activity. In the present study, the data on GT-094 was extended to measure cytokines and inflammatory proteins at the

mRNA level using RT-PCR (Fig. 8). LPS stimulation of RAW 264.7 cells was shown to produce a typical macrophage-like activation leading to induction of cytokines (TNF α , IL-6, and IL-1 β) and enzymes mediating the inflammatory response (COX-2 and iNOS), as shown by elevation of mRNA levels relative to non-induced control cells. GT-094 was observed to inhibit induction of all cytokines and iNOS in a concentration dependent manner, but to have no effect on expression of COX-2. The lack of an inhibitory effect on COX-2 expression is compatible with reports on NO-ASA (Williams et al., 2003). The observation that COX-2 mRNA levels are elevated by LPS induction in the presence and absence of GT-094 demonstrates that the anti-inflammatory actions of this drug are not simply the result of inhibition of cell growth and function.

NSAID containing hybrid drugs are anticipated to inhibit COX-2, inhibiting production of PGs. In RAW 264.7 cells, GT-094 was observed to inhibit production of PG_{D2} and PG_{E2} induced by LPS (Fig. 9). The measured IC₅₀ of 4 μ M demonstrates that the thiosalicylate pharmacophore of GT-094 delivers the anticipated COX-2 inhibitory activity, which is expected to contribute to the chemopreventive profile of GT-094 in CRC (Wang and Dubois, 2006). For comparison, the concentration dependence of the anti-inflammatory activity of GT-094 towards iNOS induction is also shown (Fig. 9B).

Induction of NQO1. To investigate structure-activity relationships for induction of detoxifying phase 2 enzymes by GT-094 and its structural components, compounds were administered to Hepa 1c1c7 cells in different concentrations and NQO1 activity was measured. The Hepa 1c1c7 cell system is commonly used to screen chemopreventive agents and potential anticarcinogens, because basal NQO1 enzyme activity is relatively low and is readily induced to measurable levels that allow comparison of efficacy and potency (Kang and Pezzuto, 2004). A standard procedure measures induction of NQO1 after incubation of agents for 48 h using 4-

bromoflavone (BF) as a positive control. (Song et al., 1999) However, comparison of the time courses for BF and GT-094 showed that GT-094 activity was maximal at 24 h (data not shown); thus, a 24 h incubation was used for assay of NQO1 activity.

Concentration dependent induction of NQO1 activity was measured for GT-094, GT-015, BECS, and for GT-103 in Hepa 1c1c7 cells (Fig. 10A). The three disulfides were equipotent, whereas GT-103, incorporating S-nitrate and NSAID moieties - but no disulfide group, induced NQO1 activity, but was less efficacious. Induction of NQO1 by ISDN was not significant, and only 1.5-fold induction of NQO1 was seen in the presence of the slow NO donor DETA/NO (Fig. 10B). The nitron radical scavenger PTIO, often referred to as a “specific trap for NO”, has been used to provide evidence for the role of NO in biochemical mechanisms. For this reason, the influence of PTIO on the induction of NQO1 by GT-094 and DETA/NO was examined (Fig. 10B). PTIO (50 μ M) was observed to lower NQO1 activity induced by GT-094 and DETA/NO, but did not reach significance (one-way ANOVA with Tukey’s post test). DETA/NO at 1.5 mM has been reported to induce NQO1, but this high concentration is not relevant to understanding the activity of GT-094 at \leq 0.1 mM.

Measurement of IC₅₀ for inhibition of Hepa 1c1c7 cell growth by GT-094, GT-015, and BECS (105 μ M, 99 μ M, and 104 μ M, respectively) allowed estimation of CI. The CD and CI values for GT-094, GT-015, and BECS were very similar: CD = 58 μ M, 67 μ M, and 57 μ M, and CI = 1.8, 1.5, and 1.8, respectively.

Activation of ARE-luciferase: The mechanism of NQO1 induction by GT-094 and related compounds was studied in HepG2-ARE-C8 cells by measuring the induction of a luciferase reporter by activation of the antioxidant/electrophile reponse element (ARE). (Kang and Pezzuto, 2004). HepG2-ARE-C8 cells are human hepatocarcinomal cell lines that have been stably transfected with the pARE-T1-luciferase construct. Luciferase induction in this cell line

reflects the ability to activate the endogenous ARE which regulates expression of many phase 2 enzymes. A good correlation between ARE-luciferase induction and NQO1 induction is usually anticipated; concentration-dependent induction of ARE-luciferase by GT-094 was indeed observed. Moreover, the time course of ARE-luciferase induction by GT-094 was compared to the benchmark chemopreventive agent, BF (Fig. 10D). Both agents were observed strongly to activate ARE giving 10-15 fold luciferase induction relative to control, with differences in time dependence at the 24 h time point.

In further experiments, the influence of PTIO was again studied; definitively, PTIO did not decrease ARE-luciferase induction by GT-094 (Fig. 10C). The biological activity of PTIO is in reality not specific for NO scavenging (Goldstein et al., 2003; Nicolescu et al., 2006), therefore the influence of the soluble guanylyl cyclase (sGC) inhibitor ODQ was examined; surprisingly, ODQ significantly increased ARE-luciferase induction by GT-094, although ODQ alone had no effect (one-way ANOVA with Tukey's post test). The MEK (MAPK/ERK kinase) inhibitor, PD 98059, was also studied, in part because of the known capability of NO to activate the MAPK-ERK (mitogen-activated protein kinase-extracellular signal-regulated kinase) pathway (Thomas et al., 2004). The MEK inhibitor was observed to give significant induction of ARE-luciferase in its own right and this effect was additive with that of GT-094 in induction of ARE-luciferase (Fig. 10C). Importantly, a similar effect of PD 98059 was reported on ARE-luciferase activity in HepG2 cells by Kong and co-workers; and further, was reported to be additive with the inductive effect of the garlic-derived diallyl trisulfide (DATS) (Chen et al., 2004).

DISCUSSION

A recent review concluded that NSAIDs and COX inhibitors reduce the incidence of colonic adenomas, but that the adverse events, including cardiovascular events and gastrotoxicity, give a risk/benefit ratio that does not support their use in CRC chemoprevention in average-risk individuals (Rostom et al., 2007). The cytoprotective effects of NO in the GI tract involve actions similar to those of PGs, for example, stimulation of mucus secretion and mucosal blood flow. Nitrates are NO mimetic drugs (Thatcher et al., 2004): thus, nitroglycerin (GTN) is able to substitute for PG action in the GI tract to counterbalance pharmacological COX inhibition (MacNaughton et al., 1989). The examination of hybrid nitrates that are NSAID prodrugs (NO-NSAIDs) was therefore a rational new approach to CRC chemoprevention (Bak et al., 1998; Bolla et al., 2005). This approach led to the NO-ASA derivative, NCX 4016, originally designed for use in pain, entering clinical trials for CRC chemoprevention (Rao et al., 2006). The cessation of these trials, reportedly because of *in vitro* genotoxicity, emphasizes the need for thorough study of molecular and structural pharmacology as a basis for optimizing nitrate drugs.

GT-094, coined an NO chimera drug because it incorporates two ancillary pharmacophores in addition to the NO mimetic nitrate group, bears comparison with NO-ASA and is a good lead compound for discovery of nitrates chemopreventive in CRC, containing ancillary pharmacophores known to have chemopreventive properties in man: an NSAID (a thiosalicylate ester (Brannigan et al., 1976; Halaschek-Wiener et al., 2000; Kapadia et al., 2000)); and a disulfide. Proof-of-principle for GT-094 was obtained in the standard animal model for CRC, the formation of ACF in the colon of rats treated with AOM carcinogen: delivered after carcinogen administration in this AOM/rat model, GT-094 reduced ACF number by 45%, reduced colon crypt proliferation by 30-69%; reduced iNOS levels by 33-67%; and elevated levels of the anti-oncogene p27 in the distal colon (Hagos et al., 2007).

In the current work, antiproliferative, anti-inflammatory activity (previously reported for GT-094 *in vivo*), and induction of cytoprotective Phase 2 gene products are studied *in vitro* for compounds that deconstruct the three component structural elements of GT-094, nitrate, NSAID, and disulfide, with the intent of understanding the contribution of each structural element to activity. The classical nitrates, GTN and ISDN, were selected for study, in addition to, ABN and BBN, which are organic nitrate elements of NO-ASA, but, without the NSAID moiety. The combination of ISDN + ASA was used, since this provides both nitrate and NSAID components. BECS contains both the disulfide and the thiosalicylate NSAID elements of GT-094; whereas GT-015 contains the disulfide and nitrate elements. Similarly, GT-947, GT-794, and GT-103 contain elements of GT-094 (Fig. 1). Finally, NONOates were used as true NO-donor control compounds (DETA/NO is a slow NO donor, $t_{1/2} \sim 20$ h; SPE/NO a moderate donor, $t_{1/2} \sim 40$ min).

GT-094 was antiproliferative in the Caco-2 human colon cancer cell line, inducing a transient G2/M phase cell cycle block (Hagos et al., 2007). Cell count measurements were used to estimate antiproliferative activity for Caco-2, HT-29, and RAW 264.7 cells, and to provide estimates of Chemopreventive Index (CI) in Hepa 1c1c7 cells. Of the component compounds tested, only the disulfides, BECS, GT-094, and GT-015 at concentrations below 100 μ M significantly inhibited cell growth (Fig. 2). Disulfides such as dipropyl disulfide (DPDS) and diallyl disulfide (DADS) have been reported to reduce ACF formation in the rat/AOM model and contribute to the chemopreventive properties of allium family botanicals (Sumiyoshi and Wargovich, 1990; Wargovich et al., 1996). It is suggested that the disulfide group of DADS contributes to the antiproliferative activity (Druesne et al., 2004; Knowles and Milner, 2003); although the allyl group appears strongly to influence NQO1 induction (Munday and Munday, 2004). DADS was reported to induce a G2/M phase cell cycle block in colon cancer cells, including Caco-2 cells (Druesne et al., 2004; Knowles and Milner, 2003; Wargovich et al.,

1996), possibly by inhibition of histone deacetylase (HDAC) activity (Suzuki et al., 2006) NCX 4016 was reported to be weakly antiproliferative in colon cancer cell lines ($165 \mu\text{M} < \text{IC}_{50} < 250 \mu\text{M}$) inducing a G2/M phase block at $250 \mu\text{M}$, whereas ASA was devoid of activity (Tesei et al., 2003).

LPS induces an inflammatory response in RAW 264.7 cells that includes expression of cytokines and of enzymes including COX-2 and iNOS. GT-094 was shown to retain NSAID activity, inhibiting LPS-induced prostaglandin synthesis, but not inhibiting COX-2 transcription (Figs 8, 9). The LPS-induced elevated COX-2 transcription was unaffected by GT-094, but GT-094 inhibited elevated iNOS and cytokine transcription. Inhibition of iNOS expression was compatible with the observed concentration dependent reduction in measured iNOS activity (Figs 6, 8). The relationship of anti-inflammatory activity to structure was studied by measuring NO_2^- as a reflection of endogenous NOS activity. GT-094, BECS, and GT-015 inhibited iNOS activity, whereas component compounds and their combination had little or no effect, demonstrating that a disulfide structural element is required for anti-inflammatory activity (Fig. 6). The NO donor, SPE/NO demonstrated the anticipated effects in RAW 264.7 cells, including a very modest inhibition of iNOS activity at higher concentration, compatible with proposed roles for NO in signaling iNOS up- and down-regulation (Connelly et al., 2003; Connelly et al., 2001). The observed concentration dependence of the activity of the true NO donor, SPE/NO, was dissimilar to that of GT-015 and GT-094, casting doubt on NO being the mediator of the effects of the nitrates observed in these cells.

A further recognized contributor to chemoprevention is induction of cytoprotective phase 2 enzymes, such as NAD(P)H-dependent quinone oxidoreductase (NQO1), in particular via activation of the antioxidant/electrophile response element (ARE), which has been reported for a number of chemopreventive agents (Prester and Talalay, 1995). The activation of the ARE and

the induction of NQO1 and luciferase activity in human liver cancer cells is anticipated for compounds, including disulfides (Song et al., 1999), that are electrophiles or oxidants towards thiol sensor proteins such as the cytosolic, thiol-rich regulatory protein Keap1 (Kelch-like ECH-associated protein 1) (Zhang and Hannink, 2003). Nitrates are also able to act as oxidizing agents, especially towards thiols; indeed, oxidation of protein thiols is likely to accompany reductive bioactivation of nitrates. There are also reports that NO itself is also able to oxidize and nitrosate Keap 1 leading to ARE activation (Buckley et al., 2007; Gao et al., 2006). However, neither ISDN, nor the NO donor DETA/NO, were observed to induce NQO1 at a comparable level to the disulfides studied herein, despite the high concentrations of NO donors used.

Theoretically, all disulfides have the potential to be electrophilic towards thiols via thiol-disulfide exchange reactions, leading to GSH depletion, oxidation of the thiol groups of redox sensor proteins, and ARE activation, but significant differences in reactivity are expected. For example, DADS was reported to induce ARE-luc in HepG2 cells twofold, whereas DPDS had no effect (both 250 μ M) (Chen et al., 2004). Chemopreventive disulfides, such as DADS, induce detoxifying phase 2 enzymes via multiple pathways converging on ARE activation, and involving, in part, the transcription factor Nrf2 (nuclear factor-erythroid 2 related factor 2), and Keap1. The disulfides that were seen to have antiproliferative and anti-inflammatory activity in the present study, GT-094, GT-015, and BECS, were assayed for NQO1 induction in Hepa 1c1c7 cells and ARE-luc induction in HepG2 cells, demonstrating concentration dependent activity at levels equal or greater than those reported for DADS (Fig. 10). The simplest rationale is that the disulfide structural element is dominant, reflecting properties similar to DADS. Addition of PTIO, commonly used as a selective NO scavenger, reduced NQO1 induction by GT-094 and DETA/NO, but not significantly. The effects of adjuvant PTIO were further examined on ARE-

luciferase induction, confirming that this “NO trap” did not reduce ARE activation by GT-094. Addition of NO/cGMP and MAPK/ERK pathway inhibitors, provided no evidence for involvement of NO in ARE activation; whereas the activity profile was fully compatible with that reported for DADS and a related trisulfide (Chen et al., 2004).

There is an extensive literature on the in vitro activity of NO-NSAID hybrid nitrates: studies have reported inhibition of Wnt signaling, disruption of NFκB function, and reduction of cyclin D₁ levels by NO-ASA. (Kashfi et al., 2002; Kaza et al., 2002; Williams et al., 2003) True NO donors, such as DETA/NO, have been observed to be antiproliferative in Caco-2 cells via inhibition of ornithine decarboxylase (Buga et al., 1998), however, in HT-29 cells, high concentrations of NO donor, or NO donor plus ASA were needed to inhibit cell growth: DETA/NO (IC₅₀ ~ 750 μM); DETA/NO + ASA (IC₅₀ at 700 μM and 375 μM) (Kashfi et al., 2005). In vitro studies on NCX 4016 have ascribed activity to sustained release of low levels of NO (Bratasz et al., 2006; Gao et al., 2005), although other studies have demonstrated NO-independent biological activity for NO-ASA (Dunlap et al., 2008; Dunlap et al., 2007; Hulsman et al., 2007). The release of intracellular NO can be addressed through application of the NO sensor paradigm pioneered by Thomas et al, who studied MCF-7 cells incubated with NO donors (Thomas et al., 2004). In the present study, protein phosphorylation was caused by GT-094 (100 μM) in a pattern similar to that produced by SPE/NO (10 μM), but not SPE/NO (100 μM), ruling out production of higher fluxes of NO from GT-094. However, it must be noted that the disulfide DADS (100 μM) also has been reported to elevate intracellular levels of pERK (Knowles and Milner, 2003).

Hybrid and chimeric drugs, by design, incorporate structural elements that provide additive or synergistic pharmacophores. GT-094 is a chimeric drug containing NSAID, NO mimetic, and disulfide pharmacophores, which like NO-NSAID drugs, has demonstrated

chemopreventive properties in animal models of CRC. Theoretically, each pharmacophore element of GT-094 could provide anti-inflammation, antiproliferation, and induction of phase 2 enzymes, however, in the variety cell lines studied, the evidence is that the disulfide structural element is the dominant contributor to all observed activity. There is no unequivocal evidence in these *in vitro* systems that the NO mimetic activity of GT-094 contributes. The combination of classical nitrates with ASA demonstrated no activity *in vitro*. Thus, the inclusion of the disulfide structural element in this NO chimera is expected to contribute strongly to the chemopreventive profile. GT-094 manifests the required NSAID activity towards prostaglandin synthesis and it is anticipated that *in vivo* the intended and invaluable gastroprotective effects of the NO mimetic nitrate will come into play.

References

- Bak AW, McKnight W, Li P, Del Soldato P, Calignano A, Cirino G and Wallace JL (1998) Cyclooxygenase-independent chemoprevention with an aspirin derivative in a rat model of colonic adenocarcinoma. *Life Sci* **62**(23):367-373.
- Bolla M, Almirante N and Benedini F (2005) Therapeutic potential of nitrate esters of commonly used drugs. *Curr Top Med Chem* **5**(7):707-720.
- Brannigan LH, Hodge RB and Field L (1976) Biologically oriented organic sulfur chemistry. 14. Antiinflammatory properties of some aryl sulfides, sulfoxides, and sulfones. *J Med Chem* **19**(6):798-802.
- Bratasz A, Weir NM, Parinandi NL, Zweier JL, Sridhar R, Ignarro LJ and Kuppusamy P (2006) Reversal to cisplatin sensitivity in recurrent human ovarian cancer cells by NCX-4016, a nitro derivative of aspirin. *Proc Natl Acad Sci U S A* **103**(10):3914-3919.
- Buckley BJ, Li S and Whorton AR (2007) Keap1 modification and nuclear accumulation in response to S-nitrosocysteine. *Free Radic Biol Med*.
- Buga GM, Wei LH, Bauer PM, Fukuto JM and Ignarro LJ (1998) NG-Hydroxy-L-arginine and nitric oxide inhibit Caco-2 tumor cell proliferation by distinct mechanisms. *Am J Physiol* **275**(4, Pt. 2):R1256-R1264.
- Chen C, Pung D, Leong V, Hebbar V, Shen G, Nair S, Li W and Kong AN (2004) Induction of detoxifying enzymes by garlic organosulfur compounds through transcription factor Nrf2: effect of chemical structure and stress signals. *Free Radic Biol Med* **37**(10):1578-1590.
- Chen C, Yu R, Owuor ED and Kong AN (2000) Activation of antioxidant-response element (ARE), mitogen-activated protein kinases (MAPKs) and caspases by major green tea polyphenol components during cell survival and death. *Arch Pharm Res* **23**(6):605-612.

- Connelly L, Jacobs AT, Palacios-Callender M, Moncada S and Hobbs AJ (2003) Macrophage endothelial nitric-oxide synthase autoregulates cellular activation and pro-inflammatory protein expression. *J Biol Chem* **278**(29):26480-26487.
- Connelly L, Palacios-Callender M, Ameixa C, Moncada S and Hobbs AJ (2001) Biphasic regulation of NF-kappa B activity underlies the pro- and anti-inflammatory actions of nitric oxide. *J Immunol* **166**(6):3873-3881.
- Corpet DE and Tache S (2002) Most effective colon cancer chemopreventive agents in rats: a systematic review of aberrant crypt foci and tumor data, ranked by potency. *Nutr Cancer* **43**(1):1-21.
- Druesne N, Pagniez A, Mayeur C, Thomas M, Cherbuy C, Duee P-H, Martel P and Chaumontet C (2004) Diallyl disulfide (DADS) increases histone acetylation and p21waf1/cip1 expression in human colon tumor cell lines. *Carcinogenesis* **25**(7):1227-1236.
- Dunlap T, Abdul-Hay S, Chandrasena RE, Hagos GK, Sinha V, Wang Z, Wang H and Thatcher GRJ (2008) Nitrates and NO-NSAIDs in cancer chemoprevention and therapy: In vitro evidence querying the NO donor functionality. *Nitric Oxide* **19**(2): 115-124.
- Dunlap T, Chandrasena RE, Wang Z, Sinha V and Thatcher GRJ (2007) Quinone formation as a chemoprevention strategy for hybrid drugs: balancing cytotoxicity and cytoprotection. *Chem Res Toxicol* **20**(12):1903-1912.
- Ford PC, Wink DA and Stanbury DM (1993) Autoxidation kinetics of aqueous nitric oxide. *FEBS Lett* **326**(1-3):1-3.
- Gao J, Kashfi K, Liu X and Rigas B (2006) NO-donating aspirin induces phase II enzymes in vitro and in vivo. *Carcinogenesis* **27**(4):803-810.

- Gao J, Liu X and Rigas B (2005) Nitric oxide-donating aspirin induces apoptosis in human colon cancer cells through induction of oxidative stress. *Proc Natl Acad Sci U S A* **102**(47):17207-17212.
- Goldstein S, Russo A and Samuni A (2003) Reactions of PTIO and carboxy-PTIO with *NO, *NO₂, and O₂-. *J Biol Chem* **278**(51):50949-50955.
- Hagos GK, Carroll RE, Kouznetsova T, Li Q, Toader V, Fernandez PA, Swanson SM and Thatcher GRJ (2007) Colon cancer chemoprevention by a novel NO chimera that shows anti-inflammatory and antiproliferative activity in vitro and in vivo. *Mol Cancer Ther* **6**(8):2230-2239.
- Halaschek-Wiener J, Wacheck V, Schlagbauer-Wadl H, Wolff K, Kloog Y and Jansen B (2000) A novel Ras antagonist regulates both oncogenic Ras and the tumor suppressor p53 in colon cancer cells. *Mol Med* **6**(8):693-704.
- Hao XP, Pretlow TG, Rao JS and Pretlow TP (2001) Inducible nitric oxide synthase (iNOS) is expressed similarly in multiple aberrant crypt foci and colorectal tumors from the same patients. *Cancer Res* **61**(2):419-422.
- Hinz B, Brune K and Pahl A (2000) Nitric oxide inhibits inducible nitric oxide synthase mRNA expression in RAW 264.7 macrophages. *Biochem Biophys Res Commun* **271**(2):353-357.
- Hulsman N, Medema JP, Bos C, Jongejan A, Leurs R, Smit MJ, de Esch IJ, Richel D and Wijtmans M (2007) Chemical insights in the concept of hybrid drugs: the antitumor effect of nitric oxide-donating aspirin involves a quinone methide but not nitric oxide nor aspirin. *J Med Chem* **50**(10):2424-2431.
- Kang YH and Pezzuto JM (2004) Induction of quinone reductase as a primary screen for natural product anticarcinogens. *Methods Enzymol* **382**:380-414.

- Kapadia GJ, Azuine MA, Takayasu J, Konoshima T, Takasaki M, Nishino H and Tokuda H (2000) Inhibition of Epstein-Barr virus early antigen activation promoted by 12-O-tetradecanoylphorbol-13-acetate by the non-steroidal anti-inflammatory drugs. *Cancer Lett* **161**(2):221-229.
- Kashfi K, Borgo S, Williams JL, Chen J, Gao J, Glekas A, Benedini F, Del Soldato P and Rigas B (2005) Positional isomerism markedly affects the growth inhibition of colon cancer cells by nitric oxide-donating aspirin in vitro and in vivo. *J Pharmacol Exp Ther* **312**(3):978-988.
- Kashfi K, Ryan Y, Qiao LL, Williams JL, Chen J, Del Soldato P, Traganos F, Rigas B and Ryann Y (2002) Nitric oxide-donating nonsteroidal anti-inflammatory drugs inhibit the growth of various cultured human cancer cells: evidence of a tissue type-independent effect. *J Pharmacol Exp Ther* **303**(3):1273-1282.
- Kaza CS, Kashfi K and Rigas B (2002) Colon cancer prevention with NO-releasing NSAIDs. *Prostaglandins Other Lipid Mediat* **67**(2):107-120.
- Knowles LM and Milner JA (2003) Diallyl disulfide induces ERK phosphorylation and alters gene expression profiles in human colon tumor cells. *J Nutr* **133**(9):2901-2906.
- MacNaughton WK, Cirino G and Wallace JL (1989) Endothelium-derived relaxing factor (nitric oxide) has protective actions in the stomach. *Life Sci* **45**(20):1869-1876.
- Maragos CM, Morley D, Wink DA, Dunams TM, Saavedra JE, Hoffman A, Bove AA, Isaac L, Hrabie JA and Keefer LK (1991) Complexes of .NO with nucleophiles as agents for the controlled biological release of nitric oxide. Vasorelaxant effects. *J Med Chem* **34**(11):3242-3247.
- Munday R and Munday CM (2004) Induction of phase II enzymes by aliphatic sulfides derived from garlic and onions: an overview. *Methods Enzymol* **382**:449-456.

- Nicolescu AC, Li Q, Brown L and Thatcher GRJ (2006) Nitroxidation, nitration, and oxidation of a BODIPY fluorophore by RNOS and ROS. *Nitric Oxide* **15**(2):163-176.
- Nicolescu AC, Zavorin SI, Turro NJ, Reynolds JN and Thatcher GRJ (2002) Inhibition of lipid peroxidation in synaptosomes and liposomes by nitrates and nitrites. *Chem Res Toxicol* **15**(7):985-998.
- Prester T and Talalay P (1995) Electrophile and antioxidant regulation of enzymes that detoxify carcinogens. *Proc Natl Acad Sci U S A* **92**(19):8965-8969.
- Prochaska HJ and Santamaria AB (1988) Direct measurement of NAD(P)H:quinone reductase from cells cultured in microtiter wells: a screening assay for anticarcinogenic enzyme inducers. *Anal Biochem* **169**(2):328-336.
- Rao CV, Reddy BS, Steele VE, Wang CX, Liu X, Ouyang N, Patlolla JM, Simi B, Kopelovich L and Rigas B (2006) Nitric oxide-releasing aspirin and indomethacin are potent inhibitors against colon cancer in azoxymethane-treated rats: effects on molecular targets. *Mol Cancer Ther* **5**(6):1530-1538.
- Rosenberg L, Louik C and Shapiro S (1998) Nonsteroidal antiinflammatory drug use and reduced risk of large bowel carcinoma. *Cancer* **82**(12):2326-2333.
- Rostom A, Dube C, Lewin G, Tsertsvadze A, Barrowman N, Code C, Sampson M and Moher D (2007) Nonsteroidal anti-inflammatory drugs and cyclooxygenase-2 inhibitors for primary prevention of colorectal cancer: a systematic review prepared for the U.S. Preventive Services Task Force. *Ann Intern Med* **146**(5):376-389.
- Song LL, Kosmeder JW, 2nd, Lee SK, Gerhauser C, Lantvit D, Moon RC, Moriarty RM and Pezzuto JM (1999) Cancer chemopreventive activity mediated by 4'-bromoflavone, a potent inducer of phase II detoxification enzymes. *Cancer Res* **59**(3):578-585.

- Sumiyoshi H and Wargovich MJ (1990) Chemoprevention of 1,2-dimethylhydrazine-induced colon cancer in mice by naturally occurring organosulfur compounds. *Cancer Res* **50**(16):5084-5087.
- Suzuki T, Kouketsu A, Itoh Y, Hisakawa S, Maeda S, Yoshida M, Nakagawa H and Miyata N (2006) Highly potent and selective histone deacetylase 6 inhibitors designed based on a small-molecular substrate. *J Med Chem* **49**(16):4809-4812.
- Tesei A, Ricotti L, Ulivi P, Medri L, Amadori D and Zoli W (2003) NCX 4016, a nitric oxide-releasing aspirin derivative, exhibits a significant antiproliferative effect and alters cell cycle progression in human colon adenocarcinoma cell lines. *Int J Oncol* **22**(6):1297-1302.
- Thatcher GRJ (2007) Organic nitrates and nitrites as stores of NO, in *Radicals for Life: the various forms of nitric oxide* (van Fassen E and Vanin A eds), Elsevier Science, Amsterdam.
- Thatcher GRJ, Nicolescu AC, Bennett BM and Toader V (2004) Nitrates and NO release: Contemporary aspects in biological and medicinal chemistry. *Free Radic Biol Med* **37**(8):1122-1143.
- Thomas DD, Espey MG, Ridnour LA, Hofseth LJ, Mancardi D, Harris CC and Wink DA (2004) Hypoxic inducible factor 1alpha, extracellular signal-regulated kinase, and p53 are regulated by distinct threshold concentrations of nitric oxide. *Proc Natl Acad Sci U S A* **101**(24):8894-8899.
- Wang D and Dubois RN (2006) Prostaglandins and cancer. *Gut* **55**(1):115-122.
- Wargovich MJ, Chen CD, Jimenez A, Steele VE, Velasco M, Stephens LC, Price R, Gray K and Kelloff GJ (1996) Aberrant crypts as a biomarker for colon cancer: evaluation of

potential chemopreventive agents in the rat. *Cancer Epidemiol Biomarkers Prev* **5**(5):355-360.

Williams JL, Nath N, Chen J, Hundley TR, Gao J, Kopelovich L, Kashfi K and Rigas B (2003) Growth inhibition of human colon cancer cells by nitric oxide (NO)-donating aspirin is associated with cyclooxygenase-2 induction and beta-catenin/T-cell factor signaling, nuclear factor-kappaB, and NO synthase 2 inhibition: implications for chemoprevention. *Cancer Res* **63**(22):7613-7618.

Yang P, Felix E, Madden T, Fischer SM and Newman RA (2002) Quantitative high-performance liquid chromatography/electrospray ionization tandem mass spectrometric analysis of 2- and 3-series prostaglandins in cultured tumor cells. *Anal Biochem* **308**(1):168-177.

Zhang DD and Hannink M (2003) Distinct cysteine residues in Keap1 are required for Keap1-dependent ubiquitination of Nrf2 and for stabilization of Nrf2 by chemopreventive agents and oxidative stress. *Mol Cell Biol* **23**(22):8137-8151.

Footnotes:

1. Research funding was provided in part by NIH grants CA-102590 and CA-121107.
2. Greg Thatcher, Dept. of Medicinal Chemistry & Pharmacognosy, College of Pharmacy, University of Illinois at Chicago, 833 S Wood St., Chicago, IL 60612; Tel: 312-355-5282; E-mail: thatcher@uic.edu

Legends for Figures

Fig. 1. Upper: Structures of compounds employed in this study compared to NO-ASA (NCX 4016 and NCX 4215) and classical nitrates (ISDN, GTN). Lower: Venn diagram showing how the study compounds dissect the component structural elements of the NO chimera GT-094 (nitrate; disulfide; NSAID).

Fig. 2. Effects of GT-094 and structural components on cell proliferation. Cell count as a function of time on incubation with test compounds normalized to 0% at time zero and 100% as DMSO vehicle control, using SRB cell staining quantified at 515 nm to estimate cell population: (A) Caco-2 cells incubated with GT-094 (solid line) or DETA/NO (dashed line) for 48 h, IC_{50} (GT-094) = $41 \pm 2 \mu\text{M}$; (B) Caco-2 cells incubated with test compounds, control (horizontal lined at 48 or 96 h), GT-015 (50 μM open at 48 or 96 h), BECS (50 μM , solid at 48 or 96 h), GT-094 (100 μM , vertical lined at 48 or 96 h); (C) HT-29 cells treated with test compounds for 48 h; (D) RAW 264.7 cells treated with test compounds for 24 h. Data show mean and s.e.m.

Fig. 3. Production of NO_2^- from test compounds in RAW 264.7 cell incubations in the absence of LPS. (A) Time course for NO_2^- production by an NO donor (SPE/NO 100 μM , open circles; 1 μM , open squares), and by nitrates (GT-015 30 μM , closed circles; GT-015 10 μM , closed triangles); (B) Comparison of NO_2^- production in RAW 264.7 cell incubations of nitrates: ISDN (with or without ASA) and GT-094 at 12 h (left bar of pair) and 24 h (right bar of pair). Data determined by Griess assay show mean and s.d. For measurement of $[\text{NO}_2^-] \geq 4 \mu\text{M}$ average error was < 4% from at least triplicate measures.

Fig. 4. Production of NO_2^- from incubation of GT-094 in RAW 264.7 cell culture supernatants to test the effect of LPS induction on denitration of GT-094. (A) Primary data on nitrite release from GT-094 incubated for 12 h in supernatants from cell cultures +/- LPS and +/- L-NAME (10 μM) as NOS inhibitor (M = media without cells; CM = supernatant; CM* = supernatant from LPS induced cells). (B) Secondary data analysis. Column A: Endogenous NO_2^- production by NOS after LPS induction. Column B: Endogenous NO_2^- production after LPS induction in the presence of L-NAME. Column C: NO_2^- production from GT-094 in media alone. Column D: NO_2^- production from GT-094 with non-induced cell supernatant. Column E: NO_2^- production from GT-094 after LPS induction. Column F: NO_2^- production from GT-094 after LPS induction from induced cells treated with L-NAME. Cells were plated for 24 h before addition of LPS or LPS + L-NAME. Supernatant was removed after a further 12 h incubation to provide reaction solutions. GT-094 (100 μM) was incubated for 12 h in these solutions before Griess assay. Data show mean and s.d. Column key: A = CM* - CM; B = CM*/L-NAME - CM*; C = M+GT094 - M; D = CM+GT094 - CM; E = CM*+GT094 - CM*; F = (CM*/L-NAME+GT094) - (CM*/L-NAME).

Fig. 5. Effect of cell density (A) and arginine depletion (B) on production of NO_2^- from GT-094 in RAW 264.7 cell culture incubation. (A) Cells were plated at densities of zero, 5×10^4 , 10×10^4 , 20×10^4 cell/well for 24 h, supernatant was replaced with FBS free media containing GT-094 (100 μM), and LPS (1 $\mu\text{g}/\text{ml}$) added after 30 min; NO_2^- was measured by Griess assay after a further 20 h incubation. (B) Cells were plated at 20×10^4 cell/well for 24 h, supernatant was replaced with FBS free media containing (open bars) or absent (solid bars) L-arginine, containing GT-094 (100 μM), and LPS (1 $\mu\text{g}/\text{ml}$) added after 30 min; NO_2^- was measured by Griess assay after a further 20 h incubation. Data show mean and S.E.M.

Fig. 6. Production of NO_2^- in cells subject to iNOS induction by LPS (1 $\mu\text{g}/\text{mL}$): (A, B) RAW 264.7 cells; (C) RAW 264.7 cells or MH-S cells. (A) Time course for NO_2^- production in the absence (open triangles) or presence of an NO donor (SPE/NO 100 μM , open circles; 1 μM , open squares;), or nitrate (GT-015 30 μM , closed circles; 10 μM , closed triangles); (B) Time course of endogenous NO_2^- production calculated by subtraction of measurements in the absence from measurements in the presence of LPS (symbols as in (A)). (C) Endogenous production of NO_2^- from incubations of test compounds with RAW 264.7 cells or MH-S cells at 24 h. Data determined by Griess assay show mean and s.d. For measurement of $[\text{NO}_2^-] \geq 4 \mu\text{M}$ average error was $< 4\%$ from at least triplicate measures.

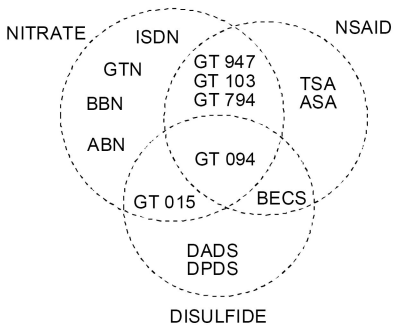
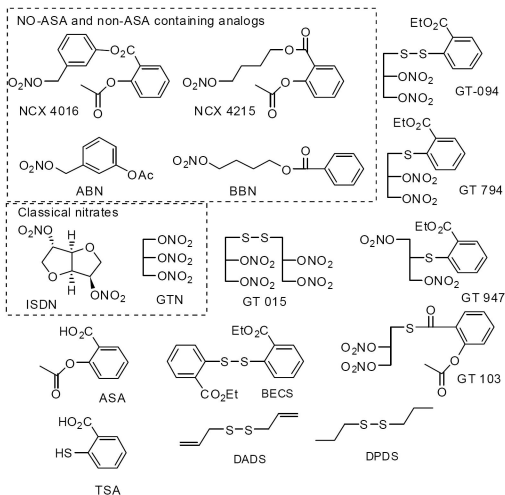
Fig. 7. Immunoblots of proteins from MCF-7 cells used to sense NO release. (A) Cells treated with the NO donor SPE/NO (100 μM) and probed with antibodies for phospho-ser15-p53 or p53 showing time dependent phosphorylation; GT-094 (100 μM) gave no p53 phosphorylation in identical experiments with GT-094. (B) Cells treated with SPE/NO (1 μM) and probed with antibodies for phospho-ERK and β -actin showing ERK phosphorylation. (C) Cells treated with GT-094 (100 μM) and probed with antibodies for phospho-ERK and total ERK showing ERK phosphorylation induced by GT-094. Representative blots from triplicate experiments are shown.

Fig. 8. The effects of GT-094 on LPS induced expression of inflammatory markers (TNF α , IL-1 β , IL-6 COX-2 and iNOS) in RAW264.7 cells measured by RT-PCR after 4 h incubation. Data quantitation and representative gel images are shown from 2-3 separate determinations.

Fig. 9. Inhibition of LPS-induced inflammatory response in RAW 264.7 cells by GT-094. Determination of PG release by LC-MS: (A) Concentration response for PG_{D2} (right axis; closed squares) and PG_{E2} (left axis; open squares); (B) Concentration response for inhibition of total PG production (PG_{D2} + PG_{E2}; solid squares; solid line; IC₅₀ = 3.9 μ M) compared to inhibition of endogenous nitrite production (open circles; dashed line; IC₅₀ = 10 μ M; measured by Griess assay).

Fig. 10. Induction of NQO1 or ARE-luciferase activity in liver cells as fold-induction relative to vehicle control. (A) Induction of NQO1 by test compounds in Hepa 1c1c7 cells after 48 h incubation; (B) Induction of NQO1 in Hepa 1c1c7 cells by GT-094, ISDN, and the NO donor DETA-NO, with and without PTIO, after 48 h; (C) Activation of ARE and induction of luciferase reporter activity in HepG2 cells by test compounds with or without pathway inhibitors measured at 20 h; (D) Time course for induction of ARE-luciferase in HepG2 cells by GT-094 (100 μ M, circles) and BF (1 μ M, triangles) versus control (squares), relative to vehicle control at time zero. Data show mean and s.e.m.

Figure 1



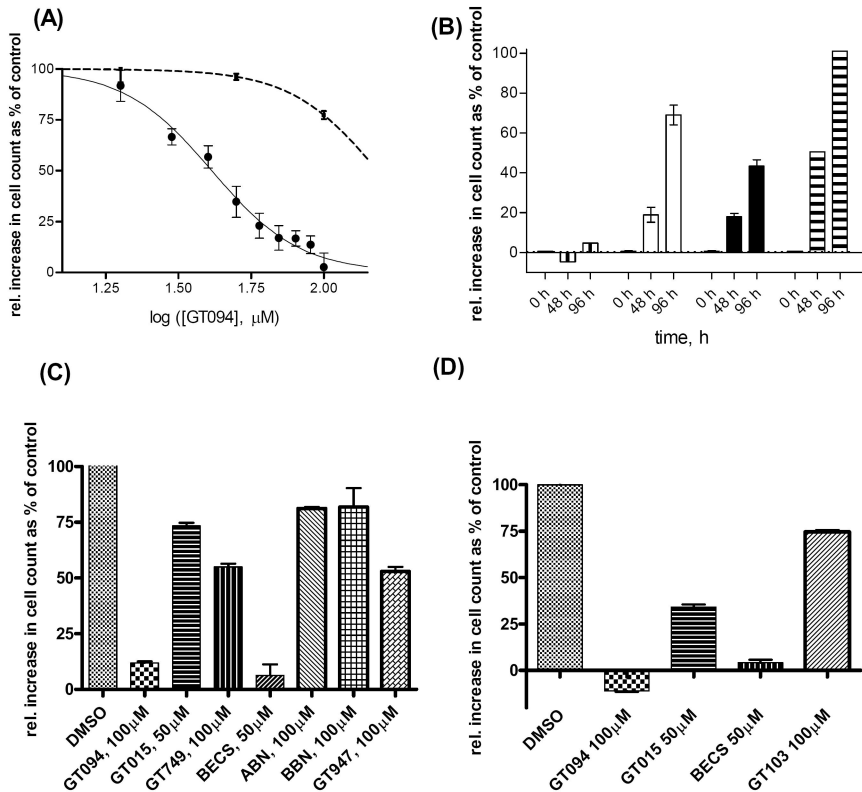


Figure 2

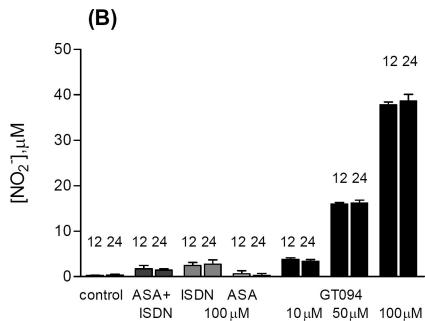
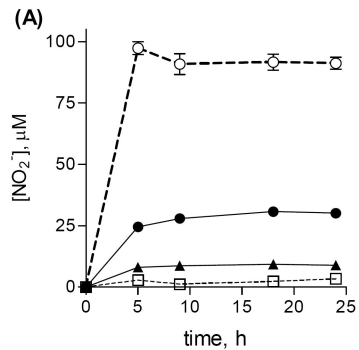


Figure 3

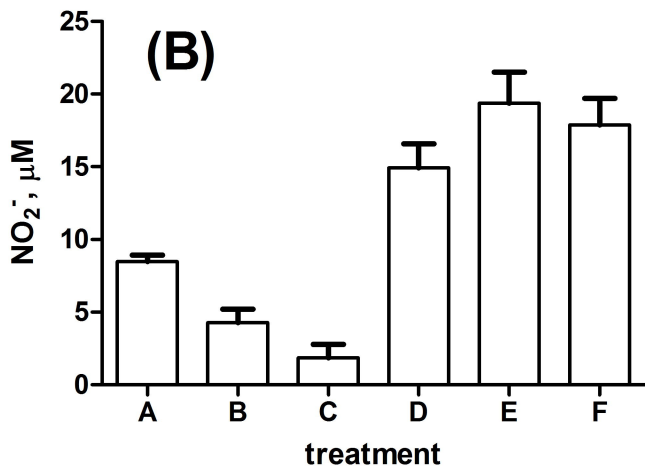
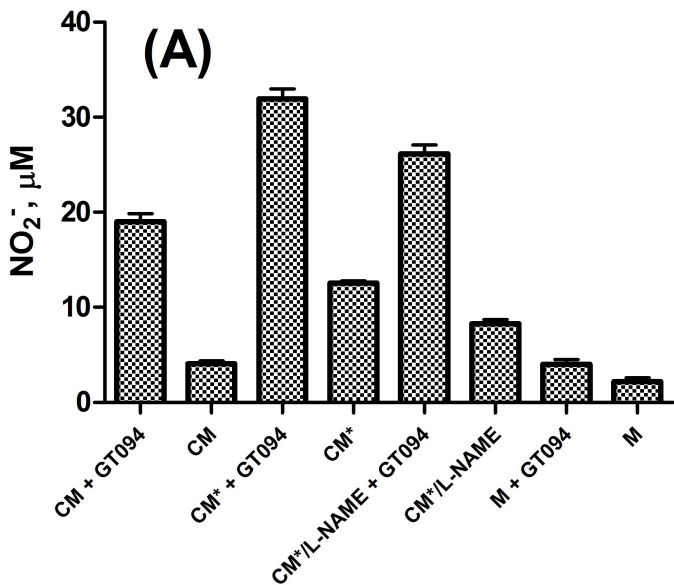
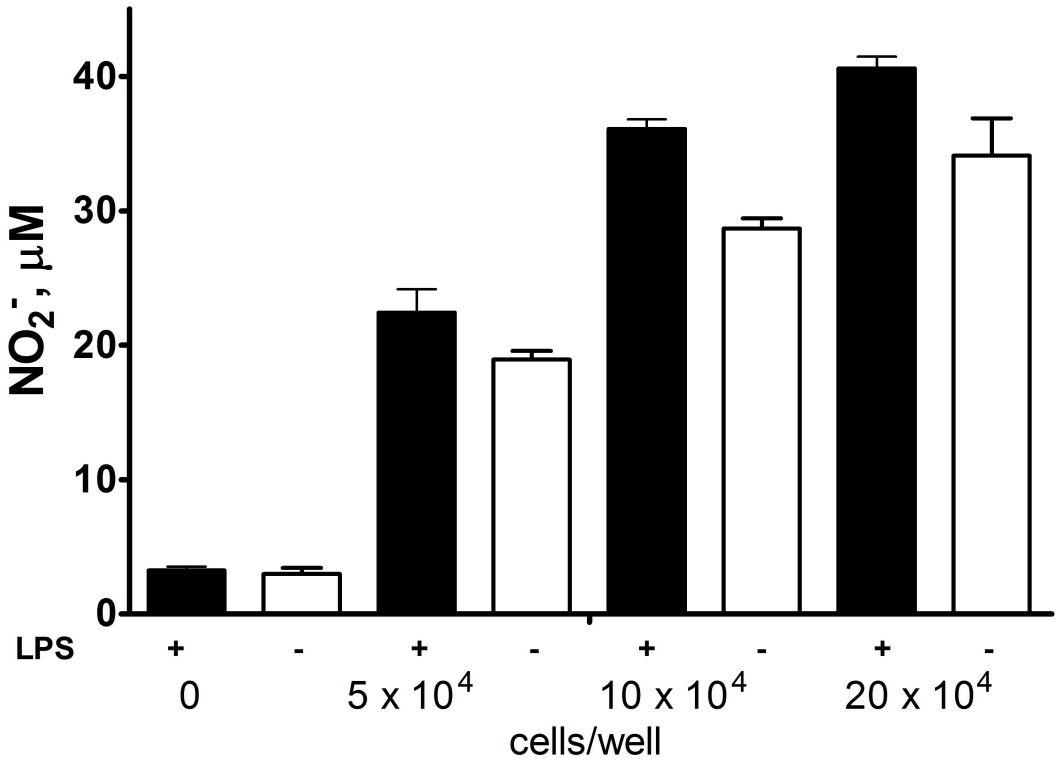


Figure 4

(A)



(B)

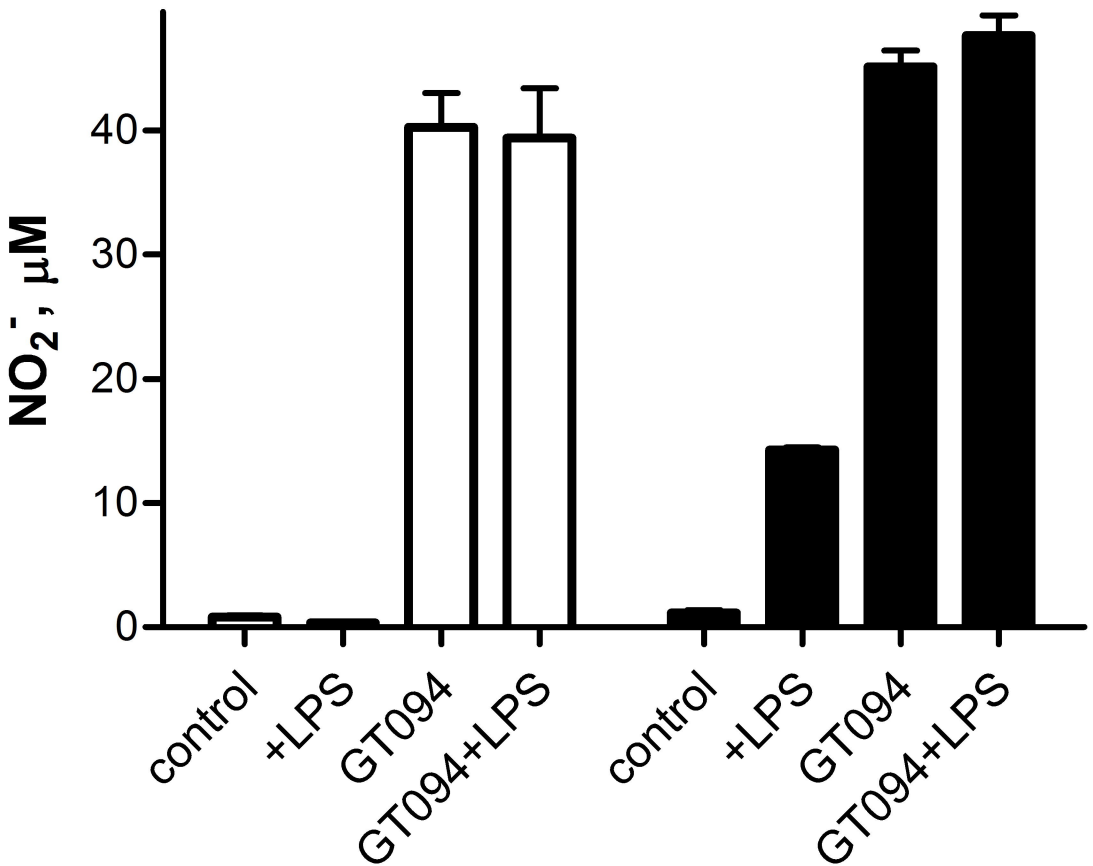


Figure 5

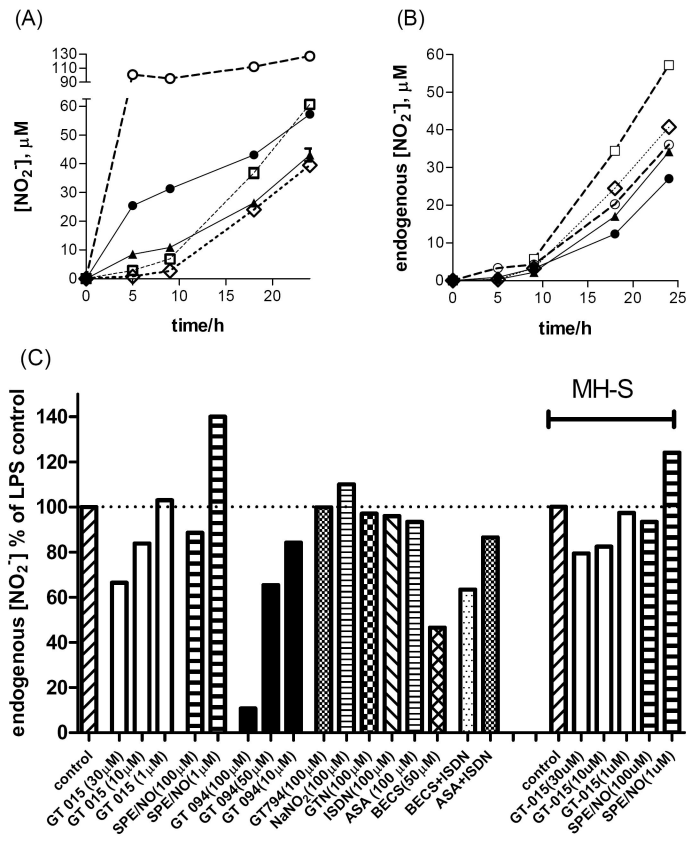


Figure 6

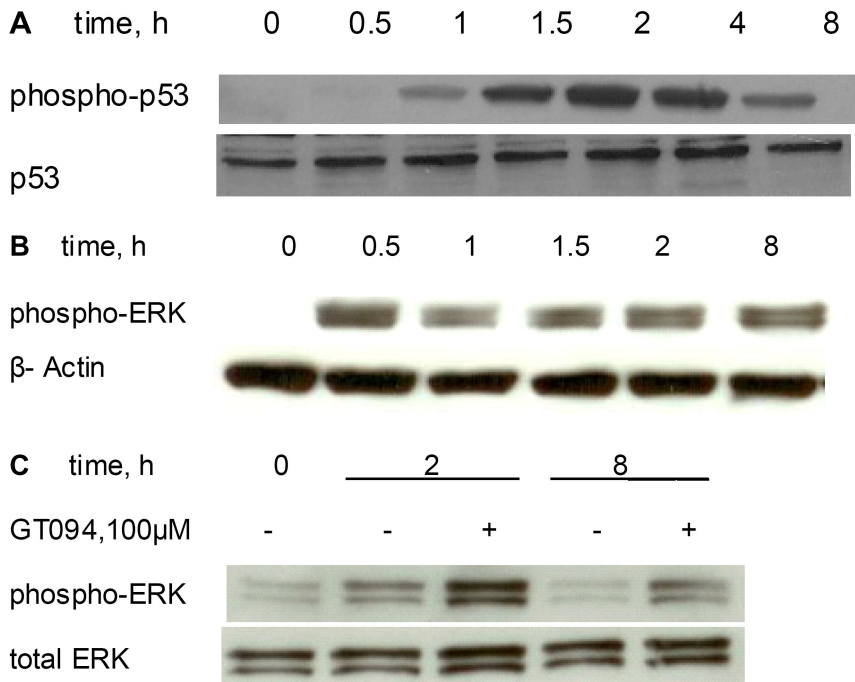


Figure 7

EXPT	1	2	3	4
LPS (1μg/mL)	-	+	+	+
GT094 (μM)	-	-	100	50

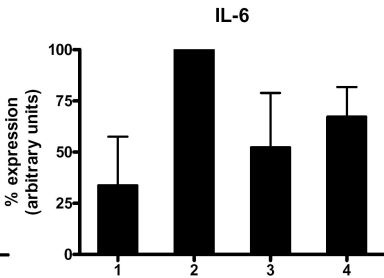
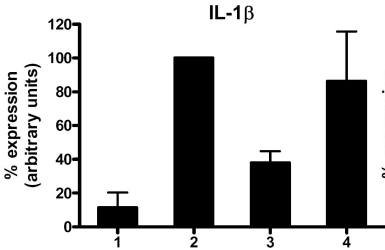
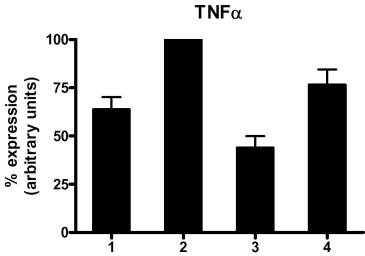
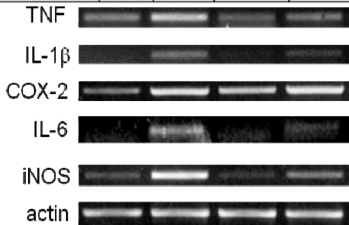


Figure 8

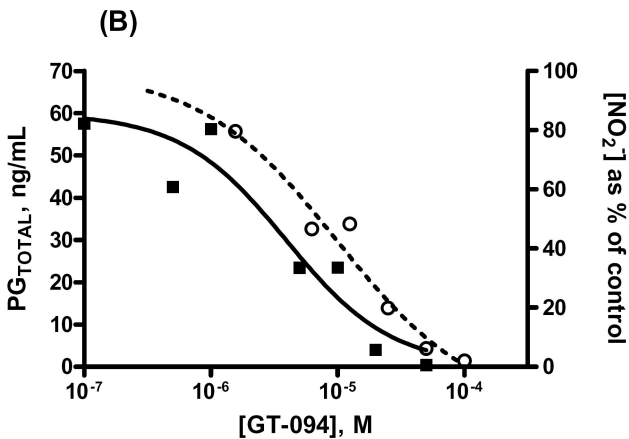
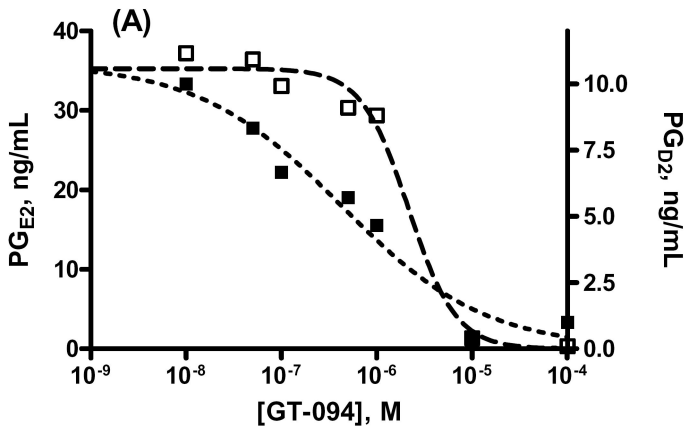


Figure 9

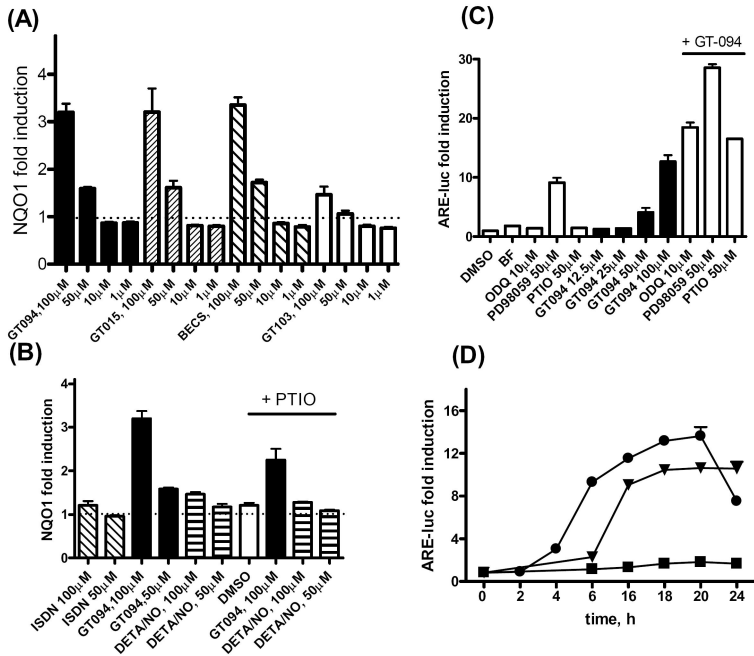


Figure 10

Anti-inflammatory, antiproliferative, and cytoprotective activity of NO chimera nitrates of use in cancer chemoprevention

Ghenet K. Hagos, Samer O. Abdul-Hay, Johann Sohn, Praneeth D. Edirisinghe, R. Esala P.
Chandrasena, Zhiqiang Wang, Qian Li, Gregory R.J. Thatcher

Department of Medicinal Chemistry & Pharmacognosy,
College of Pharmacy,
University of Illinois at Chicago,
Chicago,
IL 60612

SUPPLEMENTAL INFORMATION

MATERIALS & METHODS

Materials: All solvents and reagents used in the synthesis were purchased from Aldrich Chemical Co. (Milwaukee, WI), and were used without further purification unless otherwise noted. ^1H NMR and ^{13}C NMR spectra were recorded on a Bruker Avance 400 NMR spectrometer at 400 MHz. Chemical shift are reported in ppm (δ) using tetramethylsilane (TMS) as the internal reference and their patterns are designated as singlets (s), doublets (d), triplets (t), quartets (q), and multiplets (m). ES-MS were recorded on an Agilent 1100 LC/MSD trap. Flash column chromatography was performed using silica gel 60 (particle size 200-400 mesh) purchased from Aldrich Chemical Co, WI. Thin layer chromatography (TLC) was performed on aluminum-backed silica gel plates (Aldrich 60 F254. 200 μm in thickness). TLC plates were visualized under ultraviolet light at 254 nm, or with 5 % $\text{H}_3\text{Mo}_{12}\text{O}_{40}\text{P}$ in EtOH followed by drying with a heat gun.

Chemistry:

Preparation of GT794 and GT947: A mixture of thiosalicylic acid (5.0 g, 32.4 mmol), *p*-toluenesulfonic acid monohydrate (1.25 g, 6.55 mmol), ethanol (3.15 g, 68.5 mmol) and toluene (125 mL) was refluxed under argon for 48 h. The reaction mixture was cooled, washed with saturated sodium bicarbonate solution and brine, dried over sodium sulfate, and evaporated to give ethyl thiosalicylate. Allyl bromide (331 mg, 2.74 mmol) was dissolved in dry acetone (6 mL). Equimolar ethyl thioisalicylate was added to the reaction solution, followed by potassium carbonate (378 mg, 2.74 mmol). The mixture was then heated to reflux with stirring for 4 h. The solid was removed by filtration and the filtrate was concentrated under reduced pressure to dryness. Chromatography of the residue on silica gel chromatography with DCM/hexane (4 / 2) to gave ethyl 2-(allylthio)benzoate (398 mg). Ethyl 2-(allylthio)benzoate (398 mg, 1.79 mmol) and silver nitrate (3.59 mmol) were dissolved in dry acetonitrile (15 mL) and the resulting

reaction mixture was heated at reflux before addition of I₂ (457 mg, 1.8 mmol) in small portions over 1 h. After reflux for a further 30 min, the reaction mixture was cooled to room temperature and an aqueous solution of sodium bromide was added. The precipitate was separated by filtration and the filtrate was extracted with ethyl ether. The organic extracts were combined, washed with an aqueous solution of sodium thiosulfate in order to remove the unreacted iodine, and then concentrated in vacuo to dryness. Chromatography of the residue on silica gel column with hexane/ethyl acetate (9/1) gave GT794 and GT947 in an approximate ratio of 1:2: GT 794 (145 mg, 24%) and GT 947 (288 mg, 46%). **GT-794** ¹H NMR (CDCl₃): δ 7.96 (dd, J = 7.8 Hz, J = 1.5 Hz, 1H, Ar-H), 7.50 (td, J = 7.8 Hz, J = 1.5 Hz, 1H, Ar-H), 7.41 (dd, J = 7.8 Hz, J = 1.5 Hz, 1H, Ar-H), 7.28 (td, J = 7.8 Hz, J = 1.5 Hz, 1H, Ar-H), 5.41 (dddd, J = 8.4 Hz, J = 5.9 Hz, J = 5.5 Hz, J = 2.8 Hz, 1H, -CHONO₂), 4.93 (dd, J = 12.8 Hz, J = 2.8 Hz, 1H, -CH₂ONO₂), 4.71 (dd, J = 12.8 Hz, J = 5.9 Hz, 1H, -CH₂ONO₂), 4.38 (q, J = 7.12 Hz, 2H, -OCH₂-), 3.37 (dd, J = 14.2 Hz, J = 5.5 Hz, 1H, -SCH₂-), 3.21 (dd, J = 14.2 Hz, J = 8.4 Hz, 1H, -SCH₂-), 1.40 (t, J = 7.12 Hz, 3H, -CH₃). ¹³C NMR (CDCl₃): δ 166.3 (-CO-), 136.8, 132.5, 131.3, 127.7, 125.8, 77.3 (-CHONO₂), 69.6 (-CH₂ONO₂), 61.4 (-OCH₂-), 31.1 (-SCH₂-), 14.1 (-CH₃). ESMS: m/e 368.9 [M+Na]⁺, 384.9 [M+K]⁺. HMS calcd for [C₁₂H₁₄N₂O₈S+Na]⁺ 369.03686. Found 369.03590. **GT-947** ¹H NMR (CDCl₃): δ 7.92 (dd, J = 7.8 Hz, J = 1.5 Hz, 1H, Ar-H), 7.52 (m, 2H, Ar-H), 7.28 (ddd, J = 7.8 Hz, J = 3.2 Hz, J = 1.5 Hz, 1H, Ar-H), 4.74 (dd, J = 11.8 Hz, J = 5.1 Hz, 2H, -CH₂ONO₂), 4.66 (dd, J = 11.8 Hz, J = 7.2 Hz, 2H, -CH₂ONO₂), 4.39 (q, J = 7.16 Hz, 2H, -OCH₂-), 3.92 (dddd, J = 7.2 Hz, J = 5.1 Hz, J = 3.7 Hz, J = 2.8 Hz, 1H, -SCH-), 1.40 (t, J = 7.16 Hz, 3H, -CH₃). ¹³C NMR (CDCl₃): δ 166.5 (-CO-), 134.1, 132.4, 131.2, 130.5, 127.7, 70.6 (-CH₂ONO₂), 61.6 (-OCH₂-), 41.9 (-SCH-), 14.1 (-CH₃). ESMS: m/e 353.3 [M+Li]⁺, 368.9 [M+Na]⁺, 384.9 [M+K]⁺. HMS calcd for [C₁₂H₁₄N₂O₈S+Na]⁺ 369.03686. Found 369.03586.

Preparation of BBN (benzoyl-4-oxybutyl nitrate): BBN was prepared from 4-bromobutyl benzoate. Sodium benzoate (589 mg, 4.09 mmol) was suspended in dimethylformamide (10 mL) and after stirring for 10 min, 1,4-dibromobutane (2.736 g, 12.6 mmol) was added dropwise to the suspension. The reaction mixture was stirred at room temperature for 48 h. The reaction mixture was poured into water (100 mL) and extracted with ethyl acetate (3 x 50 mL). The organic layers were washed with water (3 x 30 mL), brine (3 x 50 mL), dried over sodium sulfate, and evaporated under reduced pressure and the residue purified by silica gel chromatography, utilizing an eluant mixture of hexane/DCM 1/1 (v/v). Appropriate fractions were collected, the solvents were evaporated under reduced pressure and the 4-bromobutyl benzoate was obtained as a yellowish oil (916 mg, 87.5%). $^1\text{H NMR}$ (CDCl_3) δ : 7.99 (dd, $J = 8.4$ Hz, $J = 1.3$ Hz, 2H, Ar-H), 7.53 (ddd, $J = 8.4$ Hz, $J = 1.3$ Hz, 1H, Ar-H), 7.16 (dd, $J = 8.4$ Hz, 2H, Ar-H), 4.40 (t, $J = 6.15$ Hz, 2H, OCH_2), 3.34 (t, $J = 6.28$ Hz, 2H, CH_2Br), 1.86-1.73 (m, 4H, CH_2CH_2).

4-Bromobutyl benzoate (916 mg, 3.58 mmol) was dissolved in anhydrous acetonitrile (20 mL) and then silver nitrate (1.84 g, 10.74 mmol) was added. The suspension was stirred at room temperature for 1 h and then refluxed gently for 14 h. The solid was filtered through celite and the solvent was removed under reduced pressure. Chromatography of the residue on a silica gel column using hexane / ether = 7:3. gave the desired 4-nitrooxybutyl benzoate (**BBN**) as an oil (736 mg, 85.9 %). $^1\text{H NMR}$ (CDCl_3): δ 8.01 (dd, $J = 8.4$ Hz, $J = 1.3$ Hz, 2H, Ar-H), 7.54 (ddd, $J = 8.4$ Hz, $J = 1.3$ Hz, 1H, Ar-H), 7.13 (dd, $J = 8.4$ Hz, 2H, Ar-H), 4.49 (t, $J = 5.8$ Hz, 2H, OCH_2), 4.33 (t, $J = 5.8$ Hz, 2H, CH_2ONO_2), 1.87 (m, 4H, CH_2CH_2). $^{13}\text{C NMR}$ (CDCl_3): δ 166.6 (CO), 133.2, 130.2, 129.6, 128.5, 72.8 (OCH_2), 64.1 (CH_2ONO_2), 25.2 (CH_2), 23.8 (CH_2). ESMS: m/e 262.0 $[\text{M}+\text{Na}]^+$, 277.9 $[\text{M}+\text{K}]^+$. HMS calcd for $[\text{C}_{11}\text{H}_{13}\text{NO}_5+\text{Na}]^+$ 262.06914. Found 262.06848.

Preparation of ABN (2-acetoxybenzyl nitrate): 3-(Bromomethyl)phenyl acetate (1.0 g, 4.38 mmol) was dissolved in anhydrous acetonitrile (20 mL) and then silver nitrate (2.25 g,

13.14 mmol) was added. The suspension was stirred at room temperature for 1 h and then refluxed gently for 4 h. The solid was filtered off through a celite pad, and the filtrate was removed under reduced pressure. Chromatography of the residue on silica gel column using hexane/ethyl acetate (3/1) gave the desired 2-(nitromethyl)phenyl acetate (**ABN**) as an oil (745 mg, 80.5 %). ^1H NMR (CDCl_3): δ 7.41 (dd, $J = 7.8$ Hz, 1H, Ar-H), 7.25 (dd, $J = 7.8$ Hz, $J = 1.1$ Hz, 1H, Ar-H), 7.14 (s, 1H, Ar-H), 7.13 (dd, $J = 7.8$ Hz, $J = 1.1$ Hz, 1H, Ar-H), 5.42 (s, 2H, $\text{ArCH}_2\text{ONO}_2$), 2.30 (s, 3H, $-\text{CH}_3$). ^{13}C NMR (CDCl_3): δ 169.2 (CO), 150.8, 133.8, 129.9, 126.1, 122.6, 122.0, 73.8 ($\text{ArCH}_2\text{ONO}_2$), 21.0 (CH_3). ESMS: m/e 234.0 $[\text{M}+\text{Na}]^+$, 250.0 $[\text{M}+\text{K}]^+$. HRMS calcd for $[\text{C}_9\text{H}_9\text{NO}_5+\text{Na}]^+$ 234.03784. Found 234.03728.

Preparation of GT-103: 3-Mercapto-1,2-dinitroxypropane (243 mg, 1.22 mmol) was dissolved in methylene chloride (5 mL) and the solution was cooled to 0 °C. *O*-Acetylsalicyloyl chloride (250 mg, 0.243 mmol) was added in one portion, followed by addition of pyridine (0.1 mL). The reaction mixture was stirred at 0 °C for one hour and complete reaction of 3-mercapto-1,2-dinitroxypropane was shown by t.l.c (DCM/hexane 3/2). The reaction mixture was poured into ice/water (100 mL) and extracted with ethyl acetate (3 x 40 mL). The organic layers were combined, dried over sodium sulfate and evaporated to dryness. Chromatography of the residue on silica gel column with methylene chloride / hexane = 3 / 2 gave the desired product as an oil (187 mg, 42.0%). ^1H NMR (CDCl_3): δ 7.91 (dd, $J = 7.8$ Hz, $J = 1.6$ Hz, 1H, Ar-H), 7.60 (ddd, $J = 7.8$ Hz, $J = 1.6$ Hz, 1H, Ar-H), 7.35 (ddd, $J = 7.8$ Hz, $J = 1.1$ Hz, 1H, Ar-H), 7.14 (dd, $J = 7.8$ Hz, $J = 1.1$ Hz, 1H, Ar-H), 5.43 (dddd, $J = 6.2$ Hz, $J = 3.1$ Hz, 1H, $-\text{CHONO}_2$), 4.81 (dd, $J = 12.9$ Hz, $J = 3.1$ Hz, 1H, $-\text{CH}_2\text{ONO}_2$), 4.62 (dd, $J = 12.9$ Hz, $J = 6.2$ Hz, 1H, $-\text{CH}_2\text{ONO}_2$), 3.46 (dd, $J = 14.6$ Hz, $J = 6.2$ Hz, 1H, $-\text{SCH}_2-$), 3.29 (dd, $J = 14.6$ Hz, $J = 6.2$ Hz, 1H, $-\text{SCH}_2-$). ^{13}C NMR (CDCl_3): δ 188.4 (ArCOS), 169.3 (COO), 148.0, 134.8, 129.5, 129.1, 126.3, 124.0, 77.4 (-

CHONO₂), 69.7 (-CH₂ONO₂), 27.8 (-SCH₂-), 21.0 (-CH₃). ESMS: m/e 382.9 [M+Na]⁺, 398.8 [M+K]⁺. HRMS calcd for [C₁₂H₁₂N₂O₉S+Na]⁺ 383.01612. Found 383.01540.

Primer Details: Sense strand TNF α , 5'-ATGAGCACAGAAAGCATGATC-3'

Antisense strand TNF α , 5'-TACAGGCTTGTCACTCGAATT-3'

Sense strand IL-1 β , 5'-TGCAGAGTTCCCCAACTGGTACATC-3'

Antisense strand IL-1 β , 5'-GTGCTGCCTAATGTCCCCTTGAATC-3'

Sense strand IL-6, 5'-GAGGATACCACTCCCAACAGACC-3'

Antisense strand IL-6, 5'-AAGTGCATCATCGTTGTTTCATACA-3'

Sense strand iNOS, 5'-AATGGCAACATCAGGTCGGCCATCACT-3'

Antisense strand iNOS, 5'-GCTGTGTGTCACAGAAGTCTCGAACTC-3'

Sense strand COX-2, 5'-GGAGAGACTATCAAGATAGT-3'

Antisense strand COX-2, 5'-ATGGTCAGTAGACTTTTACA-3'

Sense strand β -actin, 5'-ACCTTCAACACCCCAGCCATGTACG-3'

Antisense strand β -actin, 5'-CTGATCCACATCTGCTGGAAGGTGG-3'